Polymer 51 (2010) 5345–5351

Contents lists available at ScienceDirect

Polymer

journal homepage: www.elsevier.com/locate/polymer

Synthesis of TiO_2-polymer nanocomposite in supercritical CO_2 via RAFT polymerization

Behnaz Hojjati, Paul A. Charpentier*

Department of Chemical and Biochemical Engineering, University of Western Ontario, London, Ontario, Canada N6A-5B1

ARTICLE INFO

Article history:
Received 8 May 2010
Received in revised form
13 September 2010
Accepted 15 September 2010
Available online 11 October 2010

Keywords:
Grafting polymer
Kinetics
Nanocomposites

ABSTRACT

Polymer chains of PMMA were grown from nano titania (n-TiO_2) spherical surfaces by the Reversible Addition Fragmentation Chain Transfer Polymerization process (RAFT) using the green solvent, supercritical carbon dioxide ($scCO_2$). The RAFT agent (**1**), 4-cyano-4-(dodecylsulfanylthiocarbonylsulfanyl) pentanoic acid, with an available carboxyl group was first coordinated to the n-TiO_2 surface, with the S═C($SC_{12}H_{25}$) moiety subsequently used for RAFT polymerization of MMA to form the n-TiO_2/PMMA nanocomposites. The livingness of polymerization was verified using GPC, while the morphology of the nanocomposites was studied using thermogravimetric analysis (TGA), scanning electron microscopy (SEM) and dynamic light scattering (DLS). The rate of polymerization and molecular weights at different pressures in $scCO_2$ and in non-pressurized and pressurized organic solvent (THF) were compared, showing that increased CO_2 pressure provided a higher rate of polymerization and longer chain lengths indicating the utility of this approach.

1. Introduction

Reversible deactivation radical polymerization has received significant attention in recent years, as it allows production of polymers with controlled molecular weights, narrow dispersities ($Đ$), and complex macromolecular architectures [1]. In an ideal living polymerization, all chains are initiated at the beginning of the reaction; grow at the same rate, and have no termination, hence prolonging the lifetime of the propagating radicals into hours or longer [2]. As all chains possess an equal chance for growth, the molecular weight increases linearly with conversion and the dispersities $Đ$'s can be very narrow, approaching 1 [3]. Based on this technique, three main types of reversible deactivation radical polymerization have been investigated: nitroxide-mediated polymerization (NMP) [4], atom transfer radical polymerization (ATRP) [5], and reversible addition fragmentation chain transfer polymerization (RAFT) [6]. Among them, the RAFT technique provides tremendous versatility due to its ability to control the polymerization of a wide variety of monomers, including acidic monomers, without contamination by a metal catalyst [7]. The mechanism of RAFT polymerization is suggested by the CSIRO group [8] and later extensively explored by Vana et al. [9] (Scheme 1) which includes: (I) initiation, (II) pre-equilibrium involving the initial RAFT agent (CTA), (III) propagation and re-initiation, (IV) core-equilibrium, and (V) termination. However, RAFT like other living polymerizations suffers from slow rates of polymerization (R_p) requiring relatively long times for suitable chain lengths. In addition, RAFT polymerizations are generally run as a solution process, requiring organic solvents.

Supercritical carbon dioxide ($scCO_2$) has emerged as a viable "green" alternative to conventional organic solvents for accelerating reaction kinetics and limiting diffusion control in polymerization and nanotechnology [10]. CO_2 is abundant, inexpensive, non-flammable, and non-toxic, while at supercritical conditions (T_c = 31.1 °C, P_c = 7.38 MPa), CO_2 has desirable properties of both liquids and gases including a liquid-like density, a gas-like diffusivity, and a zero surface tension [11]. Its liquid-like solubility parameter and density are easily "tunable" by varying the pressure and/or temperature according to the particular polymerization conditions required. In addition, the separation of CO_2 from the liquid or solid polymer product can be obtained simply by depressurizing. Previously, DeSimone and coworkers have shown that $scCO_2$ is a promising alternative medium for free-radical, cationic, and step-growth polymerizations, and continuous processes [12–14]. Reversible deactivation radical polymerization have also been examined as McHale et al. who polymerized styrene in $scCO_2$ via NMP [15], Xia et al. polymerized fluorinated acrylates in $scCO_2$ via ATRP [16]. while recently Gregory et al. polymerized methyl methacrylate via RAFT in $scCO_2$ [17,18]. Also the effect of stabilizer concentration, pressure and temperature on the rate of polymerization of MMA via RAFT in $scCO_2$ was studied by Jaramillo-Soto et al. [19].

* Corresponding author. Tel.: +1 519 661 3466; fax: +1 519 661 3498.
E-mail address: pcharpentier@eng.uwo.ca (P.A. Charpentier).

0032-3861/$ – see front matter © 2010 Elsevier Ltd. All rights reserved.
doi:10.1016/j.polymer.2010.09.050

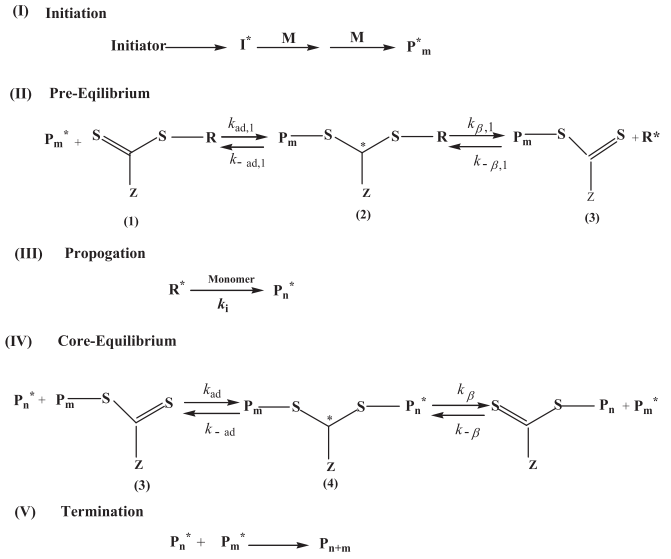

Scheme 1. Mechanism of RAFT polymerization [9].

In addition, $scCO_2$ has been already used in many nanostructure processes, such as forming ZrO_2 modified TiO_2 nanotubes [20], polymer nanocomposites [21], filling nanotubes [22], and functionalization of mesoporous silica [23]. Hasell et al. synthesized silver nanoparticle–polymer composites by supercritical CO_2 polymerization in the presence of a RAFT agent [24].

We recently reported the RAFT polymerization of acrylic acid [25] and methyl methacrylate [26] from n-TiO_2. In this paper, we report the first example of n-TiO_2/PMMA formation via RAFT polymerization in $scCO_2$, which provided significantly higher rate of polymerizations (R_p's) and number average molecular weights (M_n's) that increased with pressure, compared to polymerization in the organic solvent THF, both at ambient and pressurized conditions. The kinetics of RAFT polymerization using the direct attachment procedure was then studied, showing the polymerization maintained its "living" behavior.

2. Experimental

2.1. Materials

Titania nanospherical particles (99.5%, Sigma–Aldrich, avg. part. size D = 23.2 nm), 2, 2′-Azobis (2-methylpropionitrile) (AIBN) initiator (Toronto Research Company), were used as received. Methyl methacrylate monomer (MMA) (99%, Sigma–Aldrich, inhibited with 200 ppm BHT) was passed through an inhibitor removal column before use. The RAFT agent 4-cyano-4-(dodecylsulfanylthiocarbonylsulfanyl)pentanoic acid (**1**) was prepared as described elsewhere [27]. High purity CO_2 (from BOC Gases, 99.99% with dip-tube) was used as received.

2.2. Functionalization of n-TiO_2

0.5 g (1.28 mmol) of the RAFT agent (**1**) and 3.5 g of n-TiO_2 were dispersed in 60 ml THF with the aid of ultrasound for 1 h. The dispersed solution was then transferred to a 100 ml round bottom flask equipped with a condenser and a magnetic stirrer under nitrogen. The solution temperature was maintained at 75–78 °C under stirring for 24 h. The particles were recovered by centrifugation at 7000 rpm for 10 min. The particles were then re dissolved in THF and re-precipitated by centrifugation which was repeated until the solution was clear. The solid product was dried overnight under vacuum at 50 °C. The amount of RAFT agent anchored to the nanoparticles was determined by TGA (5.4%, i.e.100 μmol/g, which is equivalent to 1.4 #RAFT agents/nm^2) using the procedure of Yang et al. [28] while assuming the density of RAFT agent/n-TiO_2 is comparable with the density of n-TiO_2 (4.26 g/cm^3).

2.3. Synthesis of n-TiO_2/PMMA composites via RAFT in $scCO_2$ and high pressurized THF

As illustrated schematically in Scheme 2, the bifunctional RAFT agent 4-cyano-4-(dodecylsulfanylthiocarbonylsulfanyl)pentanoic acid (**1**), was used to directly coordinate to the n-TiO_2 surface, while the S=C($SC_{12}H_{25}$) moiety was used for subsequent RAFT polymerization of MMA in supercritical carbon dioxide ($scCO_2$). Synthesis was conducted in a 100 mL high-pressure stainless steel autoclave (Parr 4842) coupled with a digital pressure transducer. The stirring speed was controlled at 171 rpm. In a typical polymerization, 1.2 g of functionalized n-TiO_2 and 0.006 g AIBN were first dispersed in 25 mL methyl methacrylate with the aid of sonication. Then the solution was transferred into the reactor, purging with a flow of argon, then pumping high purity CO_2 (from BOC Gases, 99.99% with dip-tube) into the autoclave by means of a syringe pump (Isco 260D). The reactor was then heated to 70 °C, and pressurized to the desired pressure. In the case of using pressurized THF, 1.2 g of functionalized TiO_2, 25 mL methyl

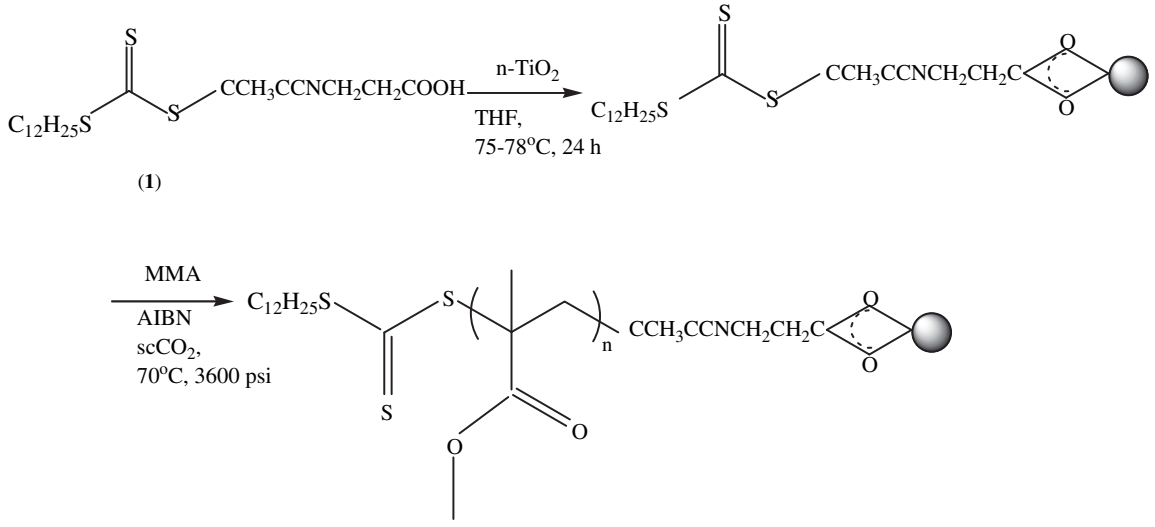

Scheme 2. Functionalization of n-TiO_2 using RAFT agent (1) and formation of n-TiO_2/PMMA nanocomposite in $scCO_2$.

Table 1
Molecular weights, *Đ*'s, and conversions of cleaved PMMA at different reaction times and different pressures. The concentration of MMA and RAFT agent is 2.35 M and 1.2×10^{-5} M, respectively.

Pressure (psi)	Time (h)	M_n (g/mol)	$M_{n,theo}$ (g/mol)	$Đ$ (M_w/M_n)	Conversion (%)
3000	1	–		–	3
	5	14,000	15,100	1.3	12
	15	29,000	30,100	1.6	20
3600	1	4800	5000	1.7	4
	5	25,000	22,300	1.5	17
	15	34,000	41,000	1.4	30
	24	80,000	83,000	1.5	60
4200	1	5800	7000	1.5	7
	5	32,000	36,600	1.5	28
	15	78,000	80,000	1.3	57
	24	120,000	120,100	1.5	70
THF[a]	1.5	7600	6900	2.1	3
	9	17,500	15,700	1.9	8
	15	23,500	26,600	1.6	14
THF[b]	5	16,000	16,800	1.6	7
	24	40,000	43,000	1.7	22

[a] Ambient pressure, speed of stirrer: 100 rpm.
[b] High pressurized THF to 3600 psi using N_2.

methacrylate, and 0.006 g AIBN were first dispersed in 40 mL THF. After transferring into the reactor, the solution was heated to 70 °C and pressurized to 3600 psi using high purity N_2. After the reaction, CO_2 and/or N_2 were carefully vented leaving the formed nanocomposite sample in the autoclave.

As polymers may grow in solution and not on the n-TiO_2 surface, the products were dissolved in THF to remove any PMMA homopolymer and/or un-reacted monomers using centrifugation at 7000 rpm for 10 min. The solid product was dried overnight under vacuum at 50 °C.

3. Characterization

The absolute molecular weight and dispersities *Đ*'s of PMMA were measured by gel permeation chromatography (GPC) with a Viscotek instrument (1 ml/min, at 30 °C) using triple detectors (refractive index (RI), viscometer detector (V), and light scattering (LS)) with the obtained calibration validated using PMMA standards (American Polymer Standards). For measuring molecular weights of polymer chains grown from titania surfaces, 30 mg of PMMA "grafted from" TiO_2 nanoparticles were dissolved in 1 mL of HCl (2 M) and 30 mL of THF. The solution was allowed to stir at 70 °C under reflux for 24 h. After centrifuging at 5000 rpm for 15 min, the solution was poured onto a glass plate and allowed to evaporate in a fume hood overnight. The recovered polymers were dissolved in THF for subsequent GPC analysis.

Fourier transform infrared (FTIR) spectra were collected of the nanocomposites using both KBr pellet on a Bruker IFS 55 FTIR instrument attached with a mercury cadmium telluride (MCT) detector, and FTIR *in-situ* monitoring of the solution concentration in the stirred 100 mL high-pressure autoclave performed using a high-pressure immersion probe (Sentinel-Mettler Toledo AutoChem). The DiComp ATR probe consists of a diamond wafer, a gold seal and a ZnSe support/focusing element, housed in alloy C-276. The probe was attached to an FTIR spectrometer (Mettler Toledo AutoChem ReactIR 4000) via a mirrored optical conduit, connected to a computer, supported by ReactIR 2.21 software (MTAC). This system uses a 24-h HgCdTe (MCT) photoconductive detector. The light source is a glow bar from which the interferometer analyzes the spectral region from 650 to 4000 cm^{-1}. The beam splitter inside the RIR4000 is ZnSe. Scanning electron microscopy (SEM) images were recorded using a LEO 1530 instrument without gold coating at 10 kV, and thermogravimetric analysis (TGA) were performed using a Mettler TGA Q500 at a heating rate of 10 °C/min under a nitrogen atmosphere. Dynamic light scattering (DLS) was performed using a Malvern Zeta Sizer 3000 HSA at room temperature.

4. Results

4.1. RAFT polymerization of n-TiO_2/PMMA in supercritical CO_2

Table 1 provides the experimental conditions and resulting M_n's, *Đ*'s and monomer conversions for MMA polymerized from the surfaces of n-TiO_2 in supercritical carbon dioxide ($scCO_2$) and THF at ambient pressure and pressurized with nitrogen at 3600 psig in a stirred FTIR autoclave. The monomer conversions were determined by following the *in-situ* FTIR peaks (Fig. 1). The decrease in height of the peak at 1638 cm^{-1} (due to C=C stretching vibration) indicates the conversion of methyl methacrylate monomer to poly methyl methacrylate (PMMA).

As described in the introduction, in an ideal living polymerization, all chains are initiated at the beginning of the reaction, grow at

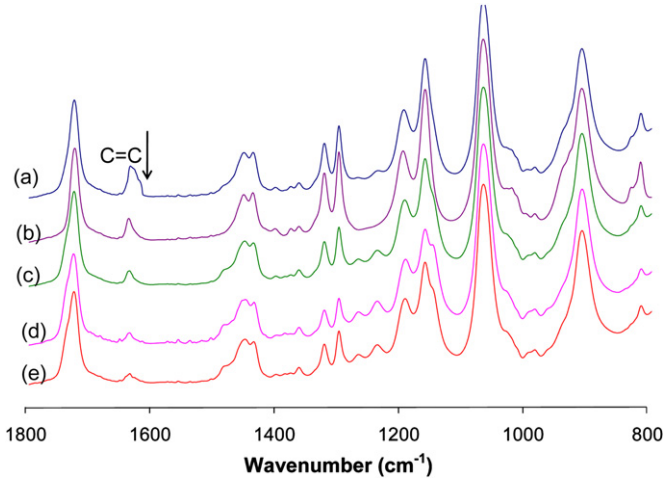

Fig. 1. *In-situ* FTIR measurement of RAFT polymerization of the n-TiO_2/PMMA composites synthesized at 70 °C and 3600 psi in $scCO_2$. Reaction time: (a) 5 min; (b) 30 min; (c) 300 min; (d) 900 min; (e) 1440 min.

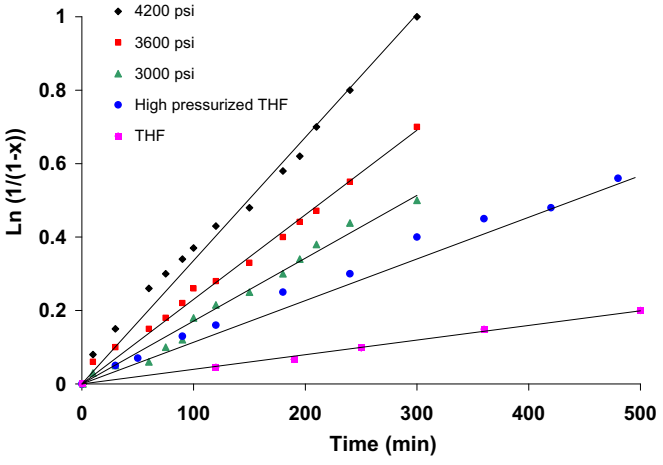

Fig. 2. First-order kinetic plot for the graft polymerization of MMA at 70 °C with AIBN initiator mediated with functionalized n-TiO_2 at different pressures of $scCO_2$ and in high pressurized and ambient pressure of THF (3600 psi) and using the surface density of 100 μmol/g.

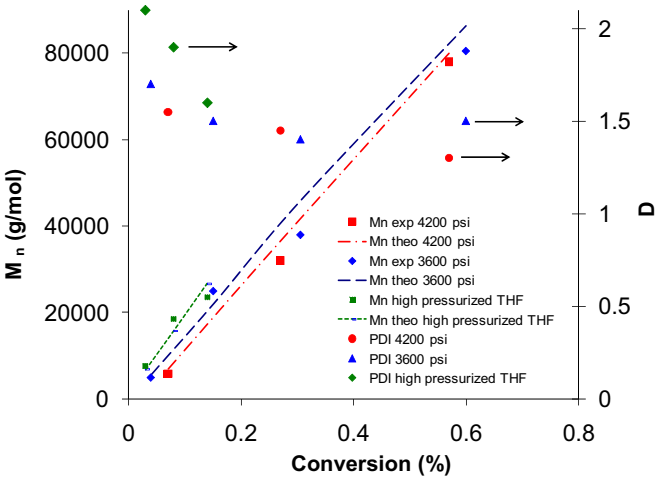

Fig. 3. Molecular weight vs. conversion data for graft polymerization of MMA from n-TiO_2 via RAFT at 70 °C and 3600 psi and 4200 psi in $scCO_2$ and in high pressurized THF at 70 °C and 3600 psi. Theoretical M_n's (——) were calculated with Equation (1).

the same rate, and proceed with no termination step. As a result, the molecular weights increase linearly with polymerization time (or monomer conversion) and the $Đ$'s can be very narrow [8]. In order to measure the molecular weights and determine whether the 'grafting from' polymerization was still living in $scCO_2$ when the RAFT agent had been attached to the n-TiO_2 surface, after depressurization of $scCO_2$ at the examined polymerization times, the PMMA chains were cleaved from the nano surface for subsequent GPC analysis. Table 1 shows that the M_n values of the cleaved PMMA samples increase directly with polymerization time for all experimental conditions. As the $scCO_2$ pressure is increased, the M_n's directly increased with pressure and significantly higher M_n's were obtained in $scCO_2$ compared to those synthesized in THF at ambient pressure and at 3600 psi, pressurized using N_2. Fig. 2 plots the monomer conversion vs. polymerization time, showing that the kinetics follow first-order behavior in regards to monomer consumption in $scCO_2$. The R_p also increases directly with increasing pressure of $scCO_2$, with significantly higher conversions being observed at given polymerization times in $scCO_2$ compared to high pressurized THF at constant temperature.

It has been shown that in RAFT polymerization, M_n can be calculated according to Equation (1) [29]:

$$M_n = \frac{[M]_o \cdot x \cdot M_{n,\text{monomer}}}{[\text{RAFT}]} \quad (1)$$

where $[M]_o$, x, $M_{n,\text{monomer}}$, and [RAFT] are the initial concentration of monomer at time = 0, the monomer conversion, the molecular weight of the monomer, and the concentration of RAFT agent attached to the surface of n-TiO_2, respectively. Fig. 3 summarizes how M_n (experimental and theoretical) changes with conversion at 3600 psi, 4200 psi in $scCO_2$, and in pressurized THF at 3600 psi with N_2. It can be clearly seen that M_n increases linearly with conversion both in high pressurized THF and in $scCO_2$, almost perfectly matching the theoretical M_n values.

It is clear that this direct coordination method for attaching the RAFT agent onto the n-TiO_2 surface provides the establishment of a steady state polymerization with reasonably high molecular weights following first-order kinetics.

In order to better understand the nature of this precipitation polymerization process in $scCO_2$, experiments were carried out in a 10 mL view cell reactor with sapphire windows. Fig. 4a shows that when RAFT agent (**1**) was dissolved in $scCO_2$ under typical polymerization conditions, a yellow transparent homogeneous phase was formed indicating solubility in $scCO_2$. Fig. 3b shows that a single opaque phase is observed in which the n-TiO_2/PMMA nanoparticles are dispersed homogeneously in $scCO_2$ during polymerization with no observation of significant clumping.

4.2. Nanocomposite characterization

The formed n-TiO_2/PMMA nanocomposites were further characterized by TGA, SEM and DLS to provide further insight into the polymerization process and nanocomposite properties. TGA was performed on the functionalized n-TiO_2 and n-TiO_2/PMMA nanocomposites as shown in Fig. 5. A typical TGA result shows two obvious regions when the temperature was increased: the first region started from 30 °C and ended at 200 °C with a relatively small slope (due to evaporation of the entrapped water or solvent); while the second region started at 250 °C and ended at 450 °C with a large slope indicating more weight loss, and decomposition of some organic groups of the PMMA and RAFT agent components. It becomes flat again after the temperature increases over 450 °C. Higher fractions of PMMA were formed as the polymerization time increased; indicating the successful polymerization in $scCO_2$ of MMA from the RAFT functionalized n-TiO_2 surface. The weight loss of n-TiO_2/PMMA in the

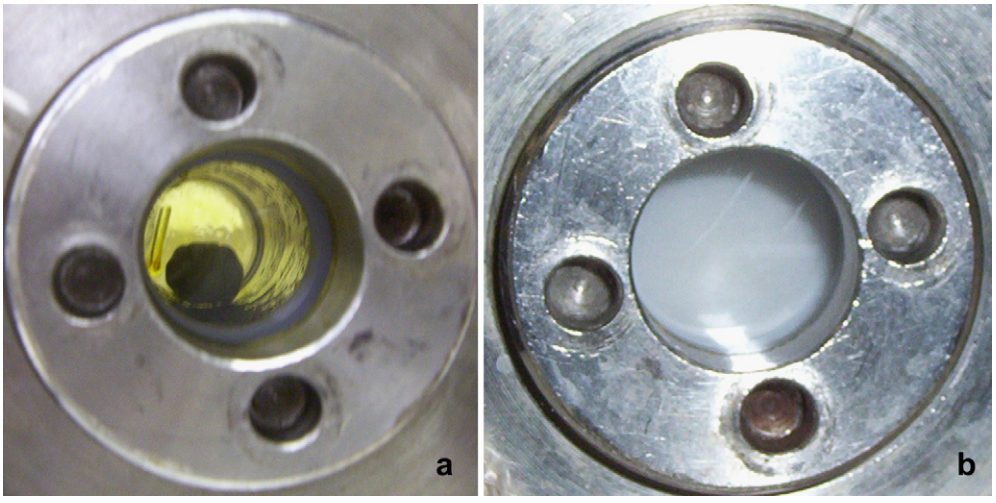

Fig. 4. Photographs following the reaction in the view cell: (a) RAFT agent (1); (b) n-TiO_2/PMMA formation at 70 °C and 3600 psi in $scCO_2$.

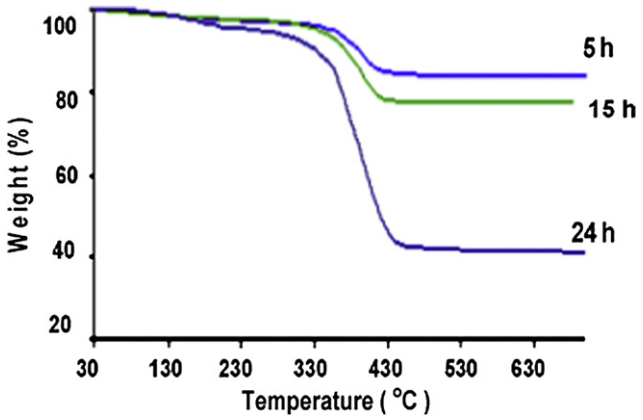

Fig. 5. TGA curves of the n-TIO$_2$/PMMA nanocomposites formed at 70 °C and 3600 psi in scCO$_2$ at different polymerization times.

region of 250–450 °C gives further evidence regarding the content and species of polymer layers grafted onto n-TiO$_2$, since the polymer and TiO$_2$ components have distinct thermal stabilities [30].

Fig. 6a presents the SEM micrographs of non-functionalized n-TiO$_2$, while Fig. 6b–d shows the n-TiO$_2$ after "grafting from" polymerization with MMA at different times in scCO$_2$, but at the same magnification. As one can see, the diameter of particles is increasing with time. These are attributed to the polymer chains that can only grow from the RAFT agent attached to the n-TiO$_2$ surface, resulting in the formation of n-TiO$_2$/PMMA nanocomposite. To more clearly examine the size of the synthesized n-TiO$_2$/PMMA nanocomposites using scCO$_2$ (at 70 °C and 3600 psi), dynamic light scattering (DLS) was utilized. The samples of nanocomposites at different times were dispersed in THF with the aid of sonication. Fig. 7 shows the particle size evolution of n-TiO$_2$/PMMA nanocomposites with respect to polymerization time. As the polymerization time increased, the mean particle size of the nanocomposites also increases, which is consistent with the SEM images. The polydispersity index (PI) as well as the intensity of the mean particle size change only slightly, indicating the continuous growth of polymer chains of PMMA with polymerization time, confirming the livingness of polymerization. Chen et al. grafted four vinyl monomers, SStNa, NaVBA, DAM, and DEA from the surface of silica via ATRP and they also found that the diameter of silica in the nanocomposites grew with the polymerization time [31].

4.3. Discussion

The results show that the polymerizations in scCO$_2$ follow living behavior, although as the nanocomposites are insoluble, the polymerization follows precipitation-type behavior. Since both supercritical and polymer phases are present in this heterogeneous media, the movement of monomer from one phase to another must be considered during the RAFT process. Based on the molecular weights summarized in Table 1, the rate of addition for each monomer of MMA to the chains of polymer in n-TiO$_2$/PMMA was calculated to be ~ 1.5–2 additions per minute; hence mass transfer limitations are considered negligible and the reaction kinetics can be assumed to control the R_p in scCO$_2$. In our previous work, the effect of RAFT concentration was studied in THF which showed that the rate of reaction decreased when increasing the concentration of RAFT agent [26]. This slow rate can be attributed to the high local concentration of RAFT agent on the surface of n-TiO$_2$ which was determined by TGA (5.4%).

As shown in Table 1, increasing pressure in THF enhanced the conversions only slightly, while pressure had a significant effect in

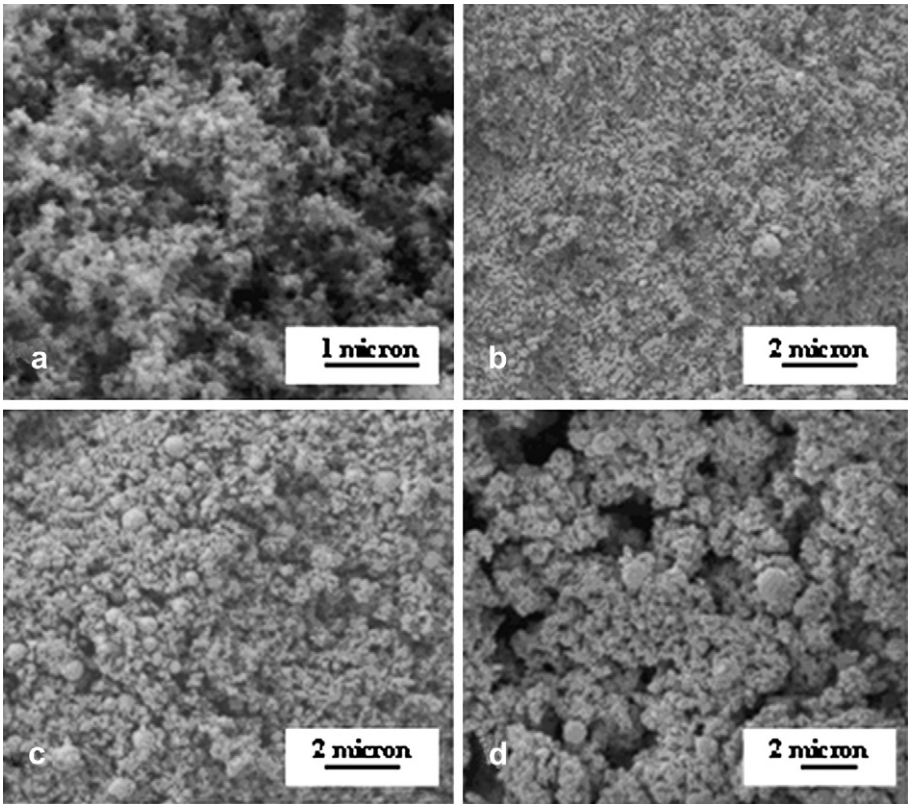

Fig. 6. SEM of (a) non-functionalized n-TiO$_2$, and of n-TiO$_2$/PMMA composite at 70 °C and 3600 psi in scCO$_2$ after (b) 5, (c) 15, and (d) 24 h.

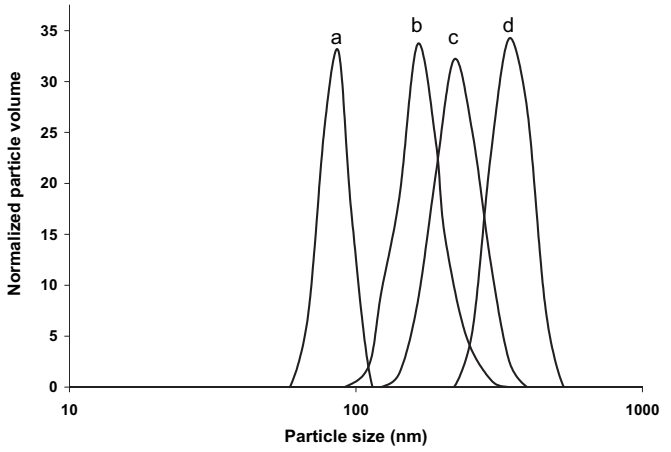

Fig. 7. Particle size distribution of the n-TiO_2/PMMA composites synthesized at 70 °C and 3600 psi in $scCO_2$ after (a) 1 h (D_{mean} = 74 nm, PI = 0.31), (b) 5 h (D_{mean} = 165 nm, PI = 0.40), (c) 15 h (D_{mean} = 266 nm, PI = 0.32), and (d) 24 h (D_{mean} = 338 nm, PI = 0.39) by DLS in THF and at room temperature.

$scCO_2$. To investigate the effect of pressure on R_p, transition state theory has been used in many studies with supercritical fluids [32,33]. In transition state theory, the following Arrhenius-type expression is used to evaluate the rate constant, k, as a function of pressure (at constant temperature) [33]:

$$k(T,p) = k(T,p_0)\exp\left(-\frac{\Delta V^{\#}}{RT}(p-p_0)\right) \quad (2)$$

where p_0, T, R, and $\Delta V^{\#}$ are the reference pressure, the absolute temperature, universal gas constant, and the activation volume, respectively. $\Delta V^{\#}$ is the change in volume in going from the reactants to the transition state. The overall reaction rate would be increased or decreased by increasing the pressure, depending on the sign of $\Delta V^{\#}$. As shown in Scheme 1 for the RAFT mechanism, the first step of the RAFT process is the decomposition of initiator (e.g. AIBN in this study). It was previously shown by DeSimone et al. that the decomposition rate of AIBN in $scCO_2$ is lower than that observed in organic solvents such as benzene at the same temperature and pressure [32]. Investigation on the pressure effects using $scCO_2$ showed that the decomposition rate and the initiation efficiency (f) of AIBN increased with increasing pressure, which increases R_p. In the propagation reaction, $\Delta V_p^{\#}$, is generally negative, (the value of $\Delta V^{\#} = -16\,cm^3\,mol^{-1}$ is reported in the literature for MMA [34]) also resulting in the R_p increasing with increasing pressure [33]. Hence, both these effects will increase the R_p and M_n values with increasing pressure, as observed experimentally. However, when performing the experiment in THF at 3600 psig, pressurized with N_2, lower conversions and M_n values were noted compared to $scCO_2$ at the same pressure. It has been previously shown that the interaction of CO_2 and the carbonyl functional group of monomers such as MMA consists of a Lewis acid and Lewis base attraction (LA–LB) between the partial positive carbon of CO_2 and the lone pairs of the carbonyl oxygen [35]. As well, the C–H···O hydrogen bond between CO_2 and the LB site has been attributed to the high solubility of polymers with a carbonyl moiety in CO_2 [36]. Hence, these interactions when using $scCO_2$ may help stabilize the transition state compared to THF.

The molecular weights and *Đ's* in Table 1 are higher than those obtained by Gregory et al. [17] who polymerized MMA in $scCO_2$ at 4000 psi and 65 °C via the RAFT technique using dithiobenzoate compounds as RAFT agents. In partial explanation, the polymerizations performed in this work occurred from n-TiO_2 surfaces, hence changing the nature of the polymerization. Gregory et al. also used alpha-cyanobenzyl dithionaphthylate as the RAFT agent, however, tertiary cyanoalkyl dithiobenzoates are likely to be better RAFT agents than the corresponding trithiocarbonates unless very low molecular weights are prepared [17].

5. Conclusions

For the first time, n-TiO_2 was functionalized with the RAFT agent, following living graft polymerization in supercritical carbon dioxide ($scCO_2$), with n-TiO_2/PMMA hybrid materials being synthesized. 4-cyano-4-(dodecylsulfanylthiocarbonylsulfanyl)pentanoic acid served both as a functionalization and living polymerization agent in $scCO_2$. SEM images, TGA, and DLS revealed the growth of the grafting polymers from n-TiO_2. This research demonstrated that living polymerization initialized from n-TiO_2 surface is promising to synthesize hybrid materials with high molecular weights. The effect of the pressure of $scCO_2$ on the rate of polymerization of MMA was investigated. GPC results of cleaved polymer after various reaction times showed that the polymerization was still living, even after the RAFT agent was directly coordinated to n-TiO_2. In addition, the kinetics of graft polymerization of MMA from the surface of n-TiO_2 in $scCO_2$ was studied and showed it was first-order in regards to monomer concentration and it was found that the rate of reaction increased with increasing the pressure of $scCO_2$.

Acknowledgements

We thank Dr. Todd Simpson of the Nanotech Laboratory, UWO for SEM analysis. This work was financially supported by the Canadian Natural Science and Engineering Research Council (NSERC).

References

[1] Jenkins AD, Jones RI, Moad G. Pure Appl Chem 2010;82:483–91.
[2] Moad G, Rizzardo E, Thang SH. Aust J Chem 2005;58:379–410.
[3] Moad G, Rizzardo E, Thang SH. Polymer 2008;49:1079.
[4] Hawker CJ, Bosman AW, Harth E. Chem Rev 2001;101:3661.
[5] Kato M, Kamigatio M, Sawamoto M, Higashimura T. Macromolecules 1995;28:1721–3.
[6] Graeme Moad G, Rizzardo E, Thang SH. Acc Chem Res 2008;41(9):1133–42.
[7] Arita T, Beuermann S, Buback M, Vana P. Macromol Mater Eng 2005;290:283.
[8] Moad G, Rizzardo E, Thang SH. Aus J Chem 2005;58:379.
[9] Vana P, Davis TP, Barner-Kowolik C. Macromol Theory Simul 2002;11:823.
[10] Johnston KP, Shah PS. Science 2004;303:482–3.
[11] Kajimoto O. Chem Rev 1999;99:355.
[12] DeSimone JM, Tumas W. Green chemistry using liquid and supercritical carbon dioxide. New York, N.Y: Oxford University Press, Inc.; 2003.
[13] Charpentier PA, Kennedy K, DeSimone JM, Roberts GW. Macromolecules 1999;32:5973–5.
[14] Kendall JL, Canelas DA, Young JL, DeSimone JM. Chem Rev 1999;99(2):543–63.
[15] MaHale R, Aldabbagh F, Zetterlund PB, Okubo M. Macromol Chem Phys 2007;208:1813–22.
[16] Xia J, Johnson T, Gaynor SG, Matyjaszewski K, DeSimone JM. Macromolecules 1999;32:4802.
[17] Gregory AM, Thurecht KJ, Howdle SM. Macromolecules 2008;41:1215.
[18] Thurecht KJ, Howdle SM. Aus J Chem 2009;62:786–9.
[19] Jaramillo-Soto G, Garcia-Moran PR, Vivaldo-Lima E. Macromol Symp 2010;289:149–54.
[20] Lucky RA, Charpentier PA. Adv Mater 2008;20:1755.
[21] Charpentier PA, Xu WZ, Li X. Green Chem 2007;9:768–76.
[22] Britz DA, Khlobystov AN, Wang J, O'Neil AS, Poliakoff M, Ardavan A, et al. Chem Commun 2004;2:176.
[23] Zemanian TS, Fryxell GE, Liu J, Mattigod S, Franz JA, Nie Z. Langmuir 2001;17:8172.
[24] Hasell T, Thurecht KJ, Jones RDW. Chem Commun 2007;38:3933–5.
[25] Hojjati B, Sui R, Charpentier PA. Polymer 2007;48:5850.
[26] Hojjati B, Charpentier PA. Polym Sci Part A Polym Chem 2008;46:3926.
[27] Ferguson CJ, Hughes RJ, Pham BTT, Hawkett BS, Gilbert RG, Serelis AK, et al. Macromolecules 2002;35:9243–5.
[28] Yang Y, Liu L, Zhang J, Li C, Zhao H. Langmuir 2007;23:2867.

[29] Chong YK, Krstina J, Le TPT, Moad G, Postma A, Rizzardo E, et al. Macromolecules 2003;36:2256–72.
[30] Khaled SM, Sui R, Charpentier PA, Rizkalla AS. Langmuir 2007;23:3988–95.
[31] Chen X, Randall DP, Perruchot C, Watts JF, Patten TE, Werne T, et al. J Colloid Interface Sci 2003;257:56.
[32] Guan Z, Combes JR, Menceloglu YZ, DeSimone JM. Macromolecules 1993;26:2663–9.
[33] Kemmere MF, Meyer T. Supercritical carbon dioxide in polymer reaction engineering. Weinheim, Germany: Willey-VCH; 2005.
[34] Odian G. Principles of polymerization. New York: John Wiley & Sons, Inc; 1981 [Chapter 3].
[35] Kazarian SG, Vincent MF, Bright FV, Liotta CL, Eckert CA. J Am Chem Soc 1996;118(7):1729–36.
[36] Raveendran P, Wallen SL. J Am Chem Soc 2002;124(42):12590–9.